Korean J. Chem. Eng., **28**(6), 1412-1419 (2011)
DOI: 10.1007/s11814-010-0527-6

Improvement of ATP regeneration efficiency and operation stability in porcine interferon-α production by *Pichia pastoris* under lower induction temperature

Minjie Gao*, Shijuan Dong, Ruisong Yu**, Jianrong Wu*, Zhiyong Zheng*, Zhongping Shi*,†, and Xiaobei Zhan***

*Key Laboratory of Industrial Biotechnology, Ministry of Education, Jiangnan University, Wuxi 214122, China
**Animal Husbandry and Veterinary Research Institute, Shanghai Academy of Agricultural Science, Shanghai Municipal Key Laboratory of Agri-Genetics and Breeding, Shanghai 201106, China
(*Received 23 October 2010 • accepted 27 December 2010*)

Abstract−The performance of traditional heterologous protein production by *Pichia pastoris* with methanol induction at 30 °C is poor, characterized by low ATP regeneration rate and weak operation stability. A low temperature induction strategy at 20 °C was thus adopted for efficient porcine interferon-α production in a 10 L fermentor. With the strategy, maximal methanol tolerance level could reach about 40 g/L to effectively deal with methanol concentration variations, so that the complicated on-line methanol measurement system could be eliminated. Moreover, metabolic analysis based on multiple state-variables measurements indicated that pIFN-α antiviral activity enhancement profited from the formation of an efficient ATP regeneration system at 20 °C induction. Compared to the induction strategy at 30 °C, the proposed strategy increased the ATP regeneration rate by 49-66%, the maximal pIFN-α antiviral activity was enhanced about 20-fold and reached a higher level of 1.5×10^6 IU/mL.

Key words: Fed-batch Culture, Fermentation, *Pichia pastoris*, Porcine Interferon-α, Protein Expression

INTRODUCTION

A heterologous protein expression system by *Pichia pastoris* has many advantages, including the ease of manipulation on the inducible alcohol oxidase (AOX) promoter to drive expression of foreign gene, the potential of growing cells to very high densities using minimal media, and the excellent nature of secreting recombinant proteins into broth for easy product purification. As a result, the methylotrophic yeast *P. pastoris* has been widely used for over-production of various heterologous proteins [1,2], including the commercially important porcine interferon-α (pIFN-α), a vaccine adjuvant capable of attenuating occurrence of porcine foot-and-mouth disease, reducing porcine reproductive, and respiratory syndrome [3,4].

Heterologous protein production by *P. pastoris* fed-batch culture is generally classified into two phases: a growth phase to accumulate a large amount of active cells with glycerol as the carbon source, followed by an induction phase by feeding methanol to initiate the expression system [5]. The standard operation mode for heterologous protein expression including pIFN-α production by *P. pastoris* is basically the suitable substrate concentration control during the two stages, while maintaining temperature at 30 °C throughout the entire fermentation [6-10]. The performance of standard protein production mode at 30 °C generally is limited by the following two factors: first, fermentation performance is strongly dependent on the formation of higher oxygen uptake rate (OUR) and thus extensive oxygen supply [11,12], heterologous protein expression by methanol induction is reported as an extremely oxygen consuming process involving ATP regeneration from NADH [13,14]; second, fermentation operation against methanol concentration variations originating from the measurement/operation mistakes such as methanol over-addition, etc., is not much stable. Excessive methanol damages the cell metabolic activity, inhibits AOX activity, and depresses protein expression [10,15]. A lower induction temperature is beneficial for efficient heterologous protein expression. The reason for this benefit is that low temperature helps to activate AOX, reduces protease secretion and thus relieves cellular component hydrolysis [16-18].

The success of industrial heterologous protein production would rely on the following: 1) increasing the carbon flux towards target protein synthesis; 2) operating the entire system with an effective ATP regeneration manner and relieving the extremely high agitation power supply; 3) allowing the fermentation system to be operated under a fault-free environment but with sufficient and variation-acceptable methanol for induction [1,19]. So far, the majority of the research work in this field mostly remains on investigating the effects of temperature and methanol induction intensity on heterologous protein titers/concentrations, while some researchers have also indicated that a higher oxygen uptake rate (OUR) is correlated with AOX activation and higher heterologous protein expression [12,20]. However, the dynamic change patterns/behaviors of several important fermentation performance indexes when the operation is subject to lower induction temperature or induction temperature shifts, such as carbon flux distribution in methanol metabolism, ATP regeneration efficiency, oxygen utilization as well as fermentation stability against outer disturbances, have been seldom reported [13, 21]. In this work, pIFN-α production at various induction temperatures was tested in a 10 L bioreactor, with the concerns focused on increasing pIFN-α activity by operating the fermentation with an efficient ATP generation way and under robust environment against the large variations in methanol concentration caused by measurement mistake or fault methanol addition.

†To whom correspondence should be addressed.
E-mail: zpshi@jiangnan.edu.cn

MATERIALS AND METHODS

1. Strain

Expression plasmid pPICZ-αIFN was constructed by ligation of pINF-α gene into pPICZα (Invitrogen, Carlsbad, CA, USA) at downstream of the promoter AOX1. pPICZ-αIFN was linearly integrated into the chromosome DNA of the host *P. pastoris* KM71 (Muts his-, PAOXII, Invitrogen, Carlsbad, CA, USA) before transformation. The recombinant *Pichia pastoris* KM71H (IFNα-pPICZαA) was constructed by Shanghai Academy of Agricultural Science, China.

2. Fermentation Medium

The details of the medium (in g/L) used and pH were as follows. Seed medium: Glucose 20, Peptone 20, Yeast extract 10. Batch medium for jar fermentor: glycerol 20, $(NH_4)_2SO_4$ 5, H_3PO_4 2 (%, v/v), $MgSO_4$ 1, $CaSO_4$ 0.1, K_2SO_4 1; PTM_1 10 (mL/L), pH 6.0.

Feeding medium for growth: glycerol 500, $(NH_4)_2SO_4$ 0.5, KH_2PO_4 0.5, $MgSO_4$ 0.03; PTM_1 10 (mL/L), pH 6.0. Feeding medium for induction: methanol 500, $(NH_4)_2SO_4$ 0.5, KH_2PO_4 0.5, $MgSO_4$ 0.03; PTM_1 10 (mL/L), pH 6.0.

3. Measurements of Cell Density and Methanol Concentration

The cell concentration was determined by measuring the optical density at 600 nm (OD_{600}), and then dry cell weight (DCW) was calculated by a consistent calibration curve of DCW versus OD_{600}. Methanol was either off-line detected by gas chromatography (GC112A, FID detector, Shanghai Precision & Scientific Instrument Co., China) with an Alpha-Col AC20 capillary column (SGE Int'l Pty. Ltd., Australia) or on-line measured by an insert-type's penetrative polymer-membrane electrode (FC-2002, Subo Co., China) supporting high temperature sterility.

4. Measurements of pINF-α Antiviral Activity and SDS-PAGE Analysis

The samples were centrifuged at 11,360 ×g for 10 min before implementing pIFN-α antiviral activity measurement and SDS-PAGE analysis. The pINF-α antiviral activity was determined according to Chinese Pharmacopoeia (Beijing, China). The procedure of pINF-α antiviral activity measurement was exactly the same as that described in the previous report [12]. As for SDS-PAGE analysis, a 20 μL sample was placed in each cell of the electrophoretic plate (15% resolving gel) with the molecular weight standards until the bromophenol blue marker had reached the bottom of the gel.

5. AOX Activity Assay

Alcohol oxidase (AOX) activity is determined using the method described by Suye et al. [22]. Samples taken from the bioreactor with accurate volume were centrifuged at 11,360 ×g for 20 min. The cells were collected and washed twice with 50 mM phosphate buffer (pH 7.5), re-centrifuged, and then re-suspended in the same buffer with the volume ratio of 1 : 1 (buffer : sample). The suspension was then sonicated (JY92-II, Scientz Biotech Co., China) at 0 °C for 10 min (pulse on, 5 s; pulse off, 10 s). The cell debris was removed by centrifugation at 4,420 ×g for 20 min, and the supernatant was used as the cell-free extract. The cell-free extract was then properly diluted by the phosphate buffer (pH 7.0) to prepare the assay solution. AOX activity was assayed with a spectrophotometer (UV-2100, Unico, China) at 500 nm by measuring the optical increase within 10 min at 37 °C, with 3 mL colorized reaction mixture consisting of 100 μmol phosphate buffer (pH 7.0), 1 μmol 4-aminoantipyrine, 4.3 μmol phenol, 10 units of peroxidase, and 200 μmol methanol, and the crude enzyme solution. One enzyme unit was defined as formation of one ìmol H_2O_2 per one minute under these conditions.

6. Porcine Interferon-α Production with Fed-batch Cultivation in a 10 L Bioreactor

The fed-batch cultivations were carried out in a 10 L standard fermentor (GUJS-10, Zhenjiang East Biotech Equipment Co., China) equipped with on-line DO/pH probes, with the initial medium volume of 5 L. The previously proposed ANNPR-Ctrl (DO/pH based artificial neural network pattern recognition control) approach [23,24] was used for feeding glycerol during growth phase to allow cells reach high density (about 110-120 g-DCW/L). The induction phase was started by feeding methanol-based medium and shifting pH from 6.0 to 5.5 at about 30 h of fermentation after glycerol was completely used up. An electronic balance (JA1102, Haikang Instrument Co., China) connected to an industrial computer via a multi-channels A/D-D/A converter (PCL-812PG, Advantech Co., Taiwan) was used to on-line monitor and calculate the methanol consumption rate by measuring the weight loss of methanol feeding reservoir. The methanol feeding was manually adjusted with a peristaltic pump (BT00-50M, Langer Co., China) to maintain methanol concentration at required set-points, by off-line measuring methanol concentration and on-line detecting methanol consumption rate. For reference, an on-line methanol electrode connected with the PC via the A/D-D/A converter was also used to drive the peristaltic pump to control methanol concentration for certain particular cases. The CO_2 and O_2 partial pressure in exhaust gas were on-line measured by a gas analyzer (LKM2000A, Lokas Co. Ltd, Korea). These data were collected by a personal computer via RS232 and then OUR and CO_2 evolution rate (CER) were calculated on-line by the standard calculation formula. After shifting into induction phase, aeration/agitation rates were fixed at 3 : 1 vvm and 900 rpm without further adjustment.

RESULTS AND DISCUSSION

1. Enhancing AOX, Metabolic & pIFN-α Activities by Lowering Induction Temperature

Fig. 1 shows the time courses of cell growth, specific methanol consumption rate, specific AOX activity and pIFN-α antiviral activity throughout the induction phase with different temperature control strategies. In the case of inducing at 20 °C (methanol concentration at 20 g/L) or maintaining methanol level at 10 g/L but induction at 30 °C, cell concentration stayed at a constant level of 110-120 g-DCW/L without significant variation during the entire induction period, regardless of the effect of dilution due to continuous methanol feeding. However, when controlling methanol concentration and temperature at 20 g/L and 30 °C, respectively, cell density decreased from 120 g-DCW/L at the beginning to 80 g-DCW/L in the end, even though the dilution effect was the lowest (the lowest methanol consumption rate) among the four cases. This indicated that the methanol toxicity had affected normal cell metabolism in this case. With the induction strategy of maintaining temperature and methanol concentration at 20 °C and 20 g/L, the specific methanol consumption rate and specific AOX activity were the highest. Maximal pIFN-α antiviral activity reached a level of 1.5×10^6 IU/mL, which was about 20-fold of the best obtained with the traditional induc-

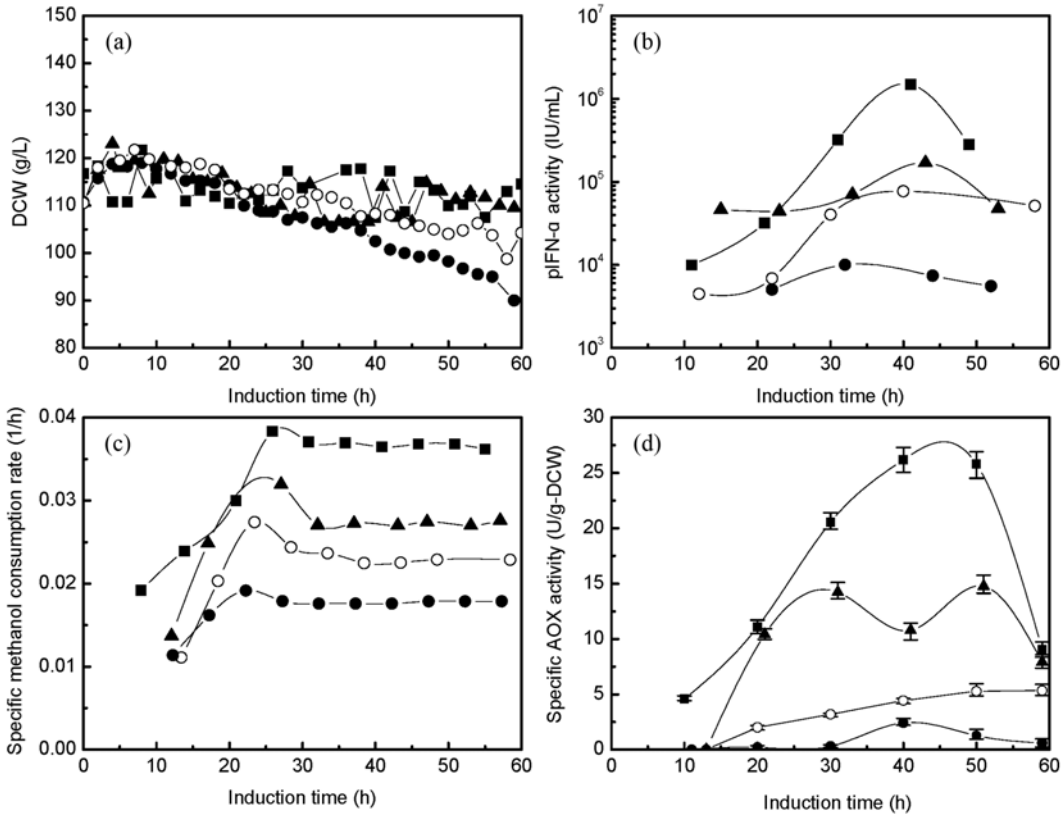

Fig. 1. Time courses of cell concentration, specific methanol consumption rate, pIFN-α antiviral activity and specific AOX activity during induction phase. ○: methanol concentration 10 g/L and 30 ºC, ■: methanol concentration 20 g/L and 20 ºC, ▲: methanol concentration 20 g/L and 25 ºC, ●: methanol concentration 20 g/L and 30 ºC.

tion strategy (30 ºC).

To further verify the effectiveness and reliability of the low temperature induction strategy, the culture broth at 30, 40 and 50 h after induction when controlling temperature at 20 ºC (methanol concentration at 20 g/L) and 30 ºC (methanol concentration at 10 g/L) was collected, analyzed and visualized by SDS-PAGE. The reason for not using supernatant obtained at the same methanol concentration (namely methanol concentration at 20 g/L, temperature at 20 ºC and 30 ºC) for the comparison is because pIFN-α antiviral activity for the latter case (methanol concentration 20 g/L and 30 ºC, as shown in Fig. 1(b)) was too low to visualize the targeted protein by SDS-PAGE. As shown in Fig. 2, a major band at 16 kDa representing pIFN-α could be observed for both cases. The bands of target protein obtained with 20 ºC induction strategy (lanes 1-3) were much more intensive than those obtained with the traditional induction method at 30 ºC (lanes A-C) at the same induction instant, which directly supported the fact that pIFN-α antiviral activity could be enhanced by lowering induction temperature.

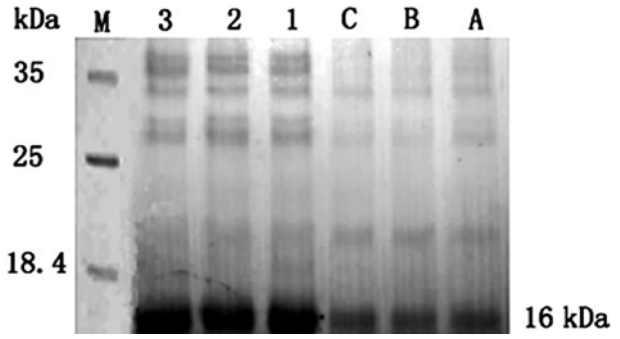

Fig. 2. SDS-PAGE analysis of the *P. pastoris* pIFN-α cultures harvested at different induction time and condition. Lane 1-3: induction time 30 h, 40 h, 50 h, at 20 ºC and methanol concentration 20 g/L; lane A-C: induction time 30 h, 40 h, 50 h, at 30 ºC and methanol concentration 10 g/L.

2. Simultaneous Enhancement of Carbon Flux Towards pIFN-α Synthesis and ATP Generation Efficiency by Lowering Induction Temperature

Heterologous protein production with *P. pastoris* is a huge oxygen consuming process, because a large amount of ATP is required for efficient heterologous protein production by utilizing the self-generated NADH with the aid of oxidative phosphorylation reaction. The potential way for achievement of an efficient pIFN-α production lies in the following three factors: 1) AOX activation to enhance the central methanol metabolism; 2) enhancement of carbon flux towards the cell and pIFN-α synthesis route; 3) acceleration of oxidative phosphorylation reaction by effectively regenerating ATP from NADH produced in the energy formation route.

Fig. 3 shows the changing patterns of OUR, CER and DO at different induction temperatures but at same methanol concentration (20 g/L). When induction temperature was reduced from 30 ºC to 20 ºC, the stable OUR after 50 h increased about 57% from 70 mmol/

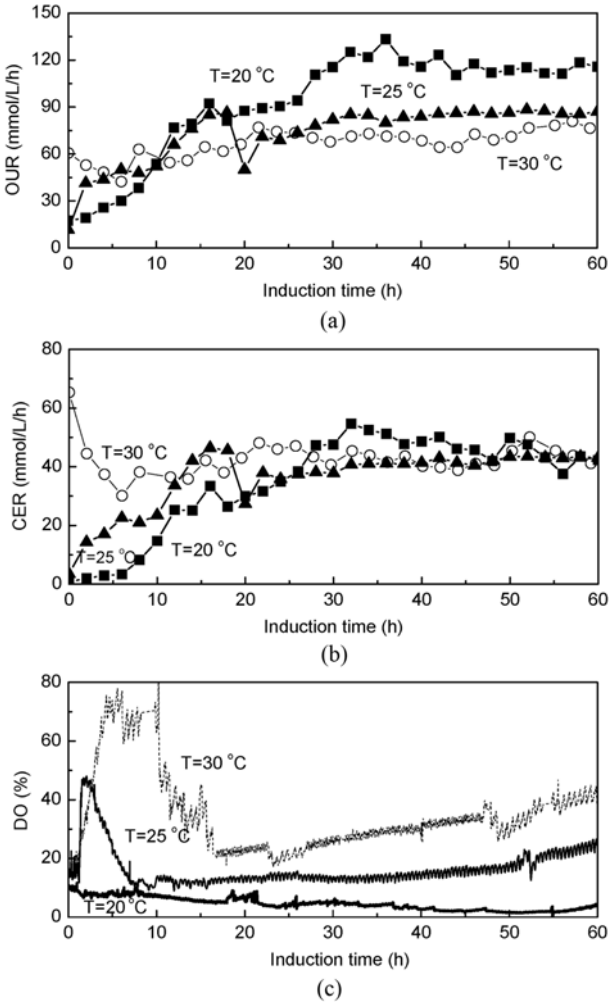

Fig. 3. The time courses of OUR, CER and DO when controlling methanol concentration at 20 g/L while maintaining temperature at different levels. ■: 20 °C, ▲: 25 °C, ○: 30 °C.

L/h to 110 mmol/L/h, while absolute CER almost remained at an equivalent level of 45 mmol/L/h. In addition, after shifting into induction phase, the recombinant *P. pastoris* must experience an adaptation period. This adaptation stage is actually inevitable because cells must require certain time to adapt the environmental change. As shown in Fig. 3, when controlling temperature at 30 °C, DO rose continuously in the first 5 h to a very high level (70%) and then stayed at this high level for another 6-7 h after starting methanol induction. DO began to decline at 12 h after induction, indicating the end of adaptation stage. On the other hand, the increase in DO quickly finished within a short period of 1 h and OUR rose immediately after initiating induction when controlling temperature at 20 °C (OUR dropped down during the first 5-6 h after induction, at 30 °C). These results implied that inducing at low induction temperature of 20 °C could largely shorten the adaptation period and was thus beneficial for improving pIFN-α's productivity.

Fig. 4 shows the simplified methanol metabolism pathway which basically consists of two metabolic pathways: a portion of formaldehyde (HCHO) generated by AOX leaves peroxisome and is further oxidized to formate (HCOOH) and eventually CO_2 (pathway A). The role of pathway A is to supply a source of energy (NADH) for

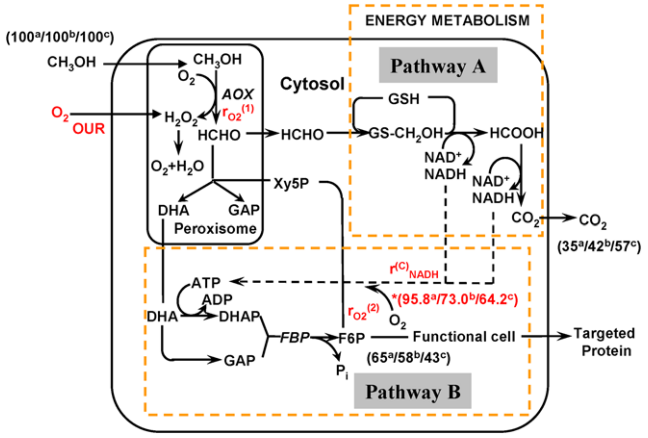

Fig. 4. Major metabolic pathways and simplified metabolic model for methanol metabolism by *P. pastoris*, when methanol concentration was controlled at 20 g/L but temperature maintained at different levels. a/b/c and *a/b/c represented carbon flux distribution in pathways A and B, and the absolute NADH consumption rate ($r^{(C)}_{NADH}$) at 20 °C, 25 °C and 30 °C after 50 h induction.

metabolism. The remaining formaldehyde is assimilated to maintain recombinant cell metabolism and thus the targeted protein synthesis by a cyclic pathway (pathway B) that starts with condensation of formaldehyde with the regenerated xylulose 5-monophosphate (Xy5P), via a series of reactions by consuming ATP regenerated [1,25]. As previously pointed out, besides AOX activation, the enhancement of carbon flux towards cell and pIFN-α synthesis route (pathway B) and effective ATP regeneration could be considered as the other dominant factors in achieving efficient heterologous protein expression with *P. pastoris* [26]. Fig. 4 shows the well-accepted and simplified metabolic model describing the methanol metabolism and relevant ATP regeneration mechanism [11,27], where ATP regeneration from TCA was not taken into account because the cells did not grow any longer during induction phase (Fig. 1(a)). As shown in Fig. 4, when temperature was decreased from 30 °C to 20 °C, carbon distribution towards pIFN-α synthesis route (pathway B) increased 51% (50 h induction). Carbon flux distribution enhancement in pathway B could promote pIFN-α synthesis. On the other hand, more ATP is required to match up with the enhanced carbon flux in pathway B.

As shown in Fig. 4, heterologous protein expression by *P. pastoris* is involved with oxygen utilization in two steps within the overall methanol metabolism. The first step is the formaldehyde (HCHO) oxidation from methanol catalyzed by AOX, which is the central and first metabolic reaction in methanol metabolism. The O_2 uptake rate in this step $r^{(1)}_{O2}$ could be determined by (on-line) measuring methanol consumption rate r_{MeOH} and utilizing the following reaction stoichiometric coefficient.

$$CH_3OH(MeOH)+\frac{1}{2}O_2 \rightarrow CH_2O+H_2O \quad (1a)$$

$$r^{(1)}_{O2}(T,t)=\frac{1}{2}r_{MeOH}(T,t) \quad (1b)$$

Here, T and t represent temperature and induction time, respectively. The second step is the oxidative phosphorylation reaction where

ATP is regenerated from NADH formed in pathway A by consuming another portion of oxygen, and the O_2 uptake rate in this step $r_{O2}^{(2)}$ could be determined by measuring methanol consumption rate r_{MeOH} and OUR, by using Eq. (2b).

$$\frac{1}{2}O_2 + NADH + (P/O)ADP \xrightarrow{P_i} (P/O)ATP + NAD^+ + H_2O \quad (2a)$$

$$r_{O2}^{(2)}(T,t) = OUR(T,t) - r_{O2}^{(1)}(T,t) = OUR(T,t) - \frac{1}{2}r_{MeOH}(T,t) \quad (2b)$$

$$r_{NADH}^{F}(T,t) = 2CER(T,t) \quad (2c)$$

$$r_{NADH}^{C}(T,t) = 2r_{O2}^{(2)}(T,t) \quad (2d)$$

$$r_{ATP}(T,t) = (P/O)r_{O2}^{(2)} = (P/O)r_{NADH}^{C}(T,t) \quad (2e)$$

Here, all of the reaction rates (r_{MeOH}, $r_{O2}^{(1)}$, $r_{O2}^{(2)}$, r_{NADH}^{F}, r_{NADH}^{C}, r_{ATP}, OUR, CER) were in mol base. $r_{NADH}^{(F)}$, $r_{NADH}^{(C)}$ and r_{ATP} represented rates of NADH formation in pathway A, NADH consumption (utilization) and ATP regeneration in the oxidative phosphorylation reaction, respectively. $r_{NADH}^{(F)}$ could be calculated using Eq. (2c) and the on-line measured CER value, as NADH formation was associated with CO_2 formation in pathway A only [11], with a reaction stoichiometric coefficient of 2 : 1.

As shown in Fig. 4, shifting temperature from 30 °C to 20 °C significantly increased the carbon distribution towards cell and pIFN-α synthesis route (pathway B), but greatly weakened the carbon flux distribution in the energy metabolism (pathway A), which could potentially decrease the self-generated NADH to be used for energizing pathway B. However, as shown in Fig. 3(b), the absolute CER almost remained unchanged under 20 °C induction, indicating that the absolute NADH formation amount or rate ($r_{NADH}^{(F)}$) in this case was almost equivalent to those when induced at 30 °C. The reason is that the absolute central carbon flux was also enhanced greatly when AOX was activated under lower induction temperature at 20 °C.

Theoretically, ATP regeneration rate r_{ATP} depends on $r_{O2}^{(2)}$ and r_{NADH}^{C} with a stoichiometric coefficient of 0.5 and 1.0, according to Eq. (2a). Furthermore, assuming P/O ratio under different induction temperatures was identical, then ATP regeneration rate r_{ATP} could be described as r_{ATP}=(P/O) r_{NADH}^{C}. Here, $r_{O2}^{(2)}$, r_{NADH}^{C}, r_{NADH}^{F} and ATP regeneration efficiency at different induction temperatures and instant

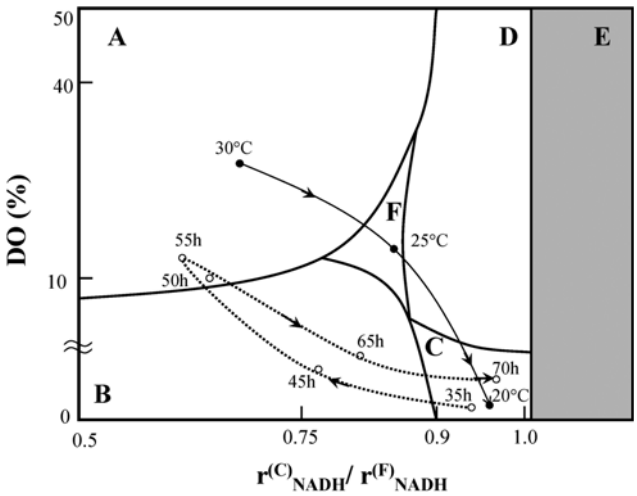

Fig. 5. A conceptional 2-D phase diagram indicating various physiological states when fermentation enters a stable induction stage. Methanol concentration was controlled at 20 g/L but temperature maintained at different levels. State A (r_{NADH}^{C}<< r_{NADH}^{F} & higher DO); State B (r_{NADH}^{C}<<r_{NADH}^{F} & lower DO); State C (r_{NADH}^{C} < r_{NADH}^{F} & r_{NADH}^{C}≈r_{NADH}^{F} & lower DO); State D (r_{NADH}^{C}<r_{NADH}^{F} & r_{NADH}^{C}≈r_{NADH}^{F} & moderate DO); State E (r_{NADH}^{C}>r_{NADH}^{F}); State F (other unidentified or transient states). Solid arrows: physiological state phase shift when inducing at 30 °C, 25 °C and 20 °C (50 h induction) for different fermentation batches; dashed arrows: physiological state phase shift when varying induction temperature in same fermentation run at 35 h and 55 h.

during three fermentation batches are summarized in Table 1. On the basis of the above assumptions, the physiological state when fermentation enters a stable induction stage could be clustered into the following six categories in a 2-D phase diagram in terms of DO and $r_{NADH}^{C}/r_{NADH}^{F}$ as shown in Fig. 5: namely, State A (r_{NADH}^{C}<<r_{NADH}^{F} & higher DO) indicating a simultaneously lower rates in NADH utilization and ATP regeneration; State B (r_{NADH}^{C}<<r_{NADH}^{F} & lower DO), a state of lower rates in both NADH consumption and ATP regeneration probably due to O_2 supply limitation; State C (r_{NADH}^{C}< r_{NADH}^{F} & r_{NADH}^{C}≈r_{NADH}^{F} & lower DO) implying a state with relatively

Table 1. Oxygen & NADH consumption rates and ATP regeneration efficiency in oxidative phosphorylation reaction under different induction temperatures and induction time

Temperature (°C)	Induction time (h)	$r_{O2}^{(2)}$ (mmol/L/h)	$r_{NADH}^{(F)}$ (mmol/L/h)	$r_{NADH}^{(C)}$ (mmol/L/h)	ATP regeneration efficiency/ increase rate (%)
30	30	29.2	87.0	58.4	67*/-
	40	29.0	85.6	58.0	68*/-
	50	32.1	92.8	64.2	69*/-
25	30	30.5	75.6	61.0	81*/-
	40	34.0	82.8	68.0	82*/-
	50	36.5	86.8	73.0	84*/-
20	30	46.1	94.8	92.2	97*/58**
	40	48.3	97.2	96.6	99*/66**
	50	47.9	99.6	95.8	96*/49**

*: ATP regeneration efficiency: $r^{(C)}_{NADH}/r^{(F)}_{NADH}$, at different induction temperature and time

**: ATP regeneration increase rate: $\{r^{(C)}_{NADH}$ (20 °C)−$r^{(C)}_{NADH}$ (30 °C)$\}/r^{(C)}_{NADH}$ (30 °C), at different induction time

higher NADH utilization and ATP regeneration rates but subject to O_2 supply limitation; State D ($r^C_{NADH}<r^F_{NADH}$ & $r^C_{NADH}\approx r^F_{NADH}$ & moderate DO), the most ideal operation mode for heterologous protein production without O_2 supply limitation; State E ($r^C_{NADH}>r^F_{NADH}$) suggesting an ill physiological state, or mistaken metabolic model; and State F specifying other unidentified or transient states.

As indicated in Table 1 and Fig. 3(c), the physiological state of *P. pastoris* under 30 °C induction could basically be categorized as State A, while that at 20 °C induction was within the region of State C. From the data in the conceptional 2-D phase diagram, physiological state phase changed when induced at different temperatures of 30 °C, 25 °C and 20 °C (50 h induction) for different fermentation batches (solid arrows, Fig. 5). It could be found that the stable physiological state gradually shifted from State A into State C via an intermediate state (State F) in this case. With the state phase shift, NADH formed in pathway A could be effectively used (higher r^C_{NADH}/r^F_{NADH}), resulting in an increased ATP regeneration efficiency. In this case (30 °C→20 °C), even though NADH formation rates r^F_{NADH} under the two induction temperatures were closed with each other, but the absolute NADH consumption rate r^C_{NADH} (representing r_{ATP}) largely increased by 49-66% (Fig. 4 and Table 1). It should be noted that State E (the ill state) never occurred in any fermentation runs as shown in Table 1 and Fig. 5, which supports the reasonableness of the metabolic model selected.

3. Enhancing Fermentation Operation Stability against Methanol Concentration Variation with Lower Induction Temperature Strategy

Methanol concentration, one of the most important parameters dominating heterologous protein production, should be strictly controlled at an adequate level. Both scarcity and excess of methanol are detrimental for pIFN-α expression. In particular, if cells were subject to high methanol concentration at 30 °C induction even for a short period, fermentation performance would irreversibly deteriorate due to severe damages of cell activity. This problem could happen if methanol was dosed excessively in occurrence of either operation or measurement mistakes. The commercially available on-line methanol electrode still has some problems such as measurement drift and response delay, which greatly limits its industrial applications. Fig. 6 shows the severe measurement response delay when using the electrode based control system for induction at 30 °C. In a test with 125 g methanol feeding into the fermentor to bring methanol concentration from 6.0 g/L up to 20.0 g/L (within 1 h during 44.5-45.5 h), the output voltage of the electrode remained at 3.0 V without any change for at least 1 h. When the output finally changed and methanol feeding stopped at 46.0 h, the methanol concentration had already reached a level of 34.0 g/L, which was more than enough to cause the "methanol toxicity" effect and fermentation failure.

Two fermentation runs were carried out intently at very high meth-

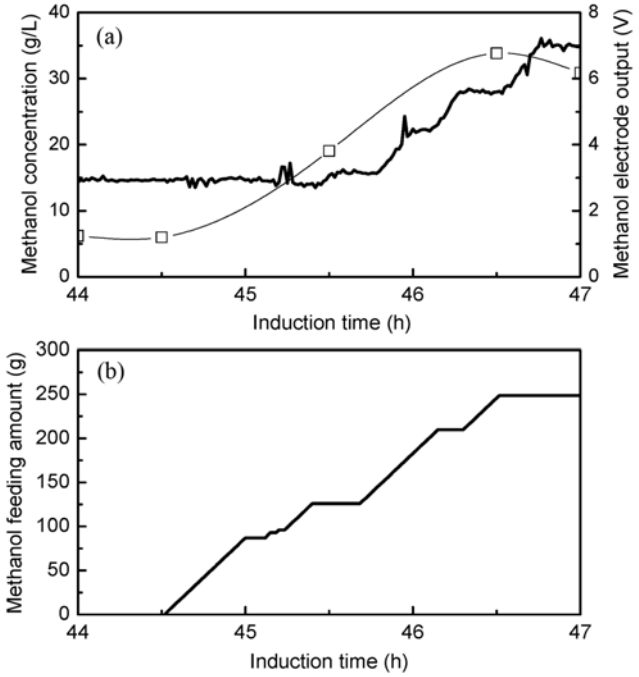

Fig. 6. Response delay features of using on-line methanol electrode based control. (a) Comparison of methanol concentration and methanol electrode output; (b) corresponding methanol feeding amount. □: methanol concentration (a), —: methanol electrode output (a); —: methanol feeding amount (b).

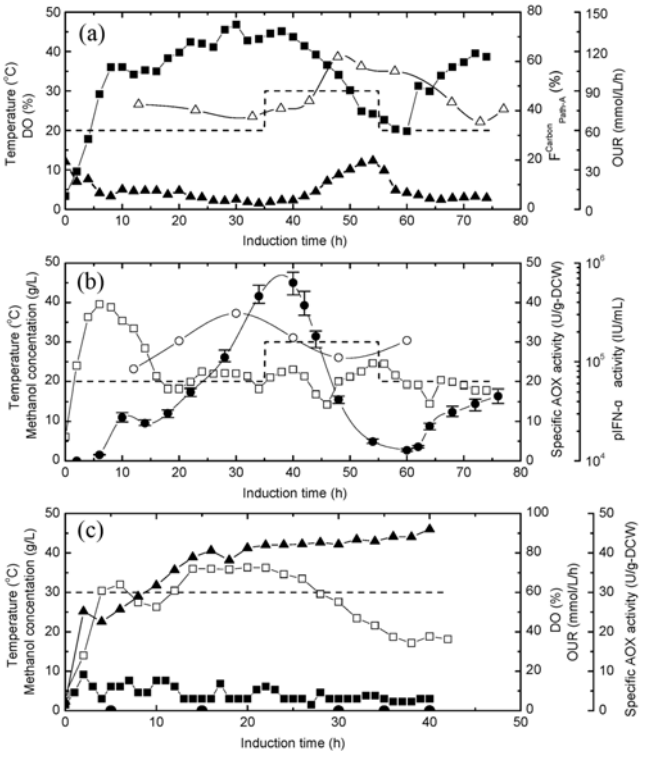

Fig. 7. Transient change patterns of DO, OUR, carbon flux distribution $F^{Cabon}_{Path\text{-}A}$ in pathway A, specific AOX activity, pIFN-α activity and methanol concentration in the fermentation processes subjected to high methanol concentration impaction in initial induction stage. (a) and (b) temperature maintained at 20 °C in the early stage but instantly varied at 35 h and 55 h; (c) temperature maintained at 30 °C without change throughout another fermentation run. ---: temperature, ▲: DO, ■: OUR, △: carbon flux distribution $F^{Cabon}_{Path\text{-}A}$ in pathway A, ●: specific AOX activity, ○: pIFN-α activity, □: methanol concentration.

anol concentration (40 g/L) during the initial induction stage (0-5 h), at 20 °C and 30 °C. As shown in Fig. 7, the maximal methanol tolerance level could reach up to 40 g/L when inducing at 20 °C. The changing patterns of DO and OUR in this case are very similar to those of controlling methanol concentration at 20 g/L and temperature at 20 °C (Fig. 3), indicating the advantages in improving fermentation stability and resistant ability against methanol concentration variation due to the measurement mistakes. This advantage would greatly simplify the industrial heterologous protein fermentation since methanol dosing still relies on human experience and knowledge in most cases [8,9]. On the other hand, the methanol tolerance ability against high methanol concentration was very weak when induced at 30 °C as no AOX activity was detected. In this case, once methanol was over-added, it could not be consumed or used any longer, causing consecutively high methanol concentration in turn. The very low OUR and high DO during 0-40 h at 30 °C induction also suggested that excessive methanol irreversibly deteriorated fermentation (Fig. 7(c)).

4. Physiological State Changes when Shifting Temperature Within Same Batch Run

The above results showed pIFN-α fermentation characteristics under various induction temperatures, suggesting that (relative) carbon flux distribution in energy metabolic pathway (pathway A) was lower at 20 °C induction, but OUR and AOX were higher. This conclusion was reached from the results originating from different fermentation batches. Considering the batch-variant nature of pIFN-α fermentation, the fermentation physiological states shifting patterns under varying induction temperature within same batch run further verified this conclusion. As shown in Fig. 7(a) and Fig. 7(b), when temperature increased from 20 °C to 30 °C at 35 h, OUR, AOX and pIFN-α activities dropped clearly, but carbon flux distribution $F_{Path\text{-}A}^{Carbon}$ in pathway A increased, with a response delay of about 5 h. When temperature dropped back from 30 °C to 20 °C at 55 h, a completely reverse result was observed. In the 2-D phase diagram of Fig. 5, with induction temperature increasing from 20 °C to 30 °C at 35 h, the physiological state of *P. pastoris* gradually shifted from State C into State A at 50 h via an intermediate state (State B), and then stayed in the region for a couple of hours. When temperature dropped back to 20 °C at 55 h, the physiological state eventually shifted back from State A into State C at 70 h again. The results indicated that the physiological state phase shift was interchangeable by manipulating the induction temperature as long as the cellular metabolic activity had not been irreversibly damaged. Both the fermentative time-transient curves (Fig. 7(a) and Fig. 7(b)) and physiological state phase transition results (Fig. 5) directly supported this conclusion.

The ideal operation mode for heterologous protein production by *P. pastoris* is to simultaneously enhance the carbon fluxes towards protein synthesis route (pathway B) and energy metabolism route (pathway A), while maintaining the highest ATP regeneration efficiency to effectively convert self-generated NADH in pathway A into ATP for energizing pathway B by manipulating DO over certain level (State D, Fig. 5). The realization of this ideal mode is difficult both theoretically and operationally. Heterologous protein production by *P. pastoris* is an extremely high oxygen consuming process, and huge power cost for rigorous agitation in large-scale fermentation would even offset the revenue obtained by the enhanced protein titer. The lower temperature induction strategy at 20 °C could improve pIFN-α production to a certain extent by enhancing the carbon flux in pIFN-α synthesis route (pathway B), fully utilizing NADH formed in energy metabolism route (pathway A) and thus resulting an increase in ATP regeneration efficiency, at the expense of weakening the carbon flux distribution in pathway A. This operation mode (State C, Fig. 5) could simultaneously improve pIFN-α production and relieve the extensive power requirement for rigorous agitation to a certain extent, and is probably the most practical choice among all possible selections. It should be noted that induction at 20 °C would also increase fermentation operation cost to some extent since cooling water (particularly for summer season) must be used. However, the cost in purifying the target protein generally accounts for about 90% of that in the entire production; therefore, it is believed that the ease of purification load caused by largely enhanced protein titers would offset the cost-up in fermentation process and promote economics of the entire protein production process.

A large number of research works have been reported concerning the effects of methanol concentration or methanol feeding strategy on protein production, the effectiveness of glycerol feeding strategies to allow the achievement of high cells density prior to methanol induction, and effects of low temperature on AOX activity, protease secretion, as well as subsequent targeted protein hydrolysis, etc. Our experimental results conducted in a 10 L bioreactor revealed that lowering induction temperature could not only stimulate AOX activity as reported, but also enhance the carbon flux in target protein

Table 2. Summarized results of 6 fermentation runs

Run #	Induction temperature (°C)	Ave. or initially loaded methanol conc. (g/L)	Adaptation period (h)	Stable specific methanol consumption rate (1/h)	Maximum $r_{NADH}^{(C)}$ (mmol/L/h)	Maximum specific AOX activity (U/g-DCW)	Maximum pIFN-α activity (IU/mL)
1	30	10	10.0	0.23	N/A[a]	5.3	7.70×10^4
2	30	20	10.0	0.18	64.2	2.4	1.00×10^4
3	25	20	8.0	0.27	73.0	14.8	1.70×10^5
4	20	20	1.0	0.37	96.6	26.2	1.49×10^6
5	20-30-20	38 (initially loaded)	1.0	N/A[a]	N/A[a]	45.0	3.09×10^5
6	30	35 (initially loaded)	-[b]	0.06	N/A[a]	0.0	0.00

[a]Not available or not detectable

[b]Fermentation completely failed due to "methanol toxicity" effect

synthesis route, ATP regeneration efficiency, and the operation stability. It should be addressed that maximal pIFN-α antiviral activity obtained in 10 L fermentor is still lower than that obtained in a smaller one (5 L with medium volume of 1.5 L); future endeavors will be continued on further increasing pIFN-α antiviral activity to approach the similar level obtained in the small fermentor. However, the experiments conducted in 10 L fermentor at least supplied some reference or information (production enhancement at same scale, operation robustness improvement, and efficient oxygen utilization) for large and industrial scale production. The major results of a total of six fermentation runs are also summarized in Table 2.

CONCLUSIONS

From the low temperature induction strategy at 20 °C conducted in a 10 L bioreactor we concluded the following: 1) maximal pIFN-α antiviral activity was enhanced about 20-fold of that obtained by traditional induction strategy at 30 °C and reached a higher level of 1.5×10^6 IU/mL; 2) inducing at lower temperature of 20 °C could enhance the carbon flux in target protein synthesis route and raise the utilization rate of self-generated NADH in an oxygen-saving mode, which directly contributes to the enhancements in ATP regeneration efficiency and pIFN-α production. Under 20 °C induction, the utilization rate of NADH increased from about 67% to 97% and absolute ATP regeneration rate 49-66% as compared to those obtained at 30 °C induction; 3) at 20 °C induction, the maximal methanol tolerance level reached a level of 40 g/L so that the operation stability against methanol concentration variations due to measurement mistakes could be enhanced even without a sophisticated online methanol measurement system. These features not only enhance pIFN-α productivity but also facilitate scale-up of the production process by relieving requirement for accurate methanol concentration control system and high oxygen supply.

ACKNOWLEDGEMENT

The authors thank the financial support from the key agricultural technology program of Shanghai Science & Technology Committee (#073919108) and Major State Basic Research Development Program (#2007CB714303), of China.

NOMENCLATURE

CER : carbon dioxide evolution rate [mmol/L/h]
DCW : dry cell weight [g/L]
DO : dissolved oxygen [%]
$F_{Path\text{-}A}^{Carbon}$: (carbon) flux distribution in metabolic pathway A [%]
OUR, r_{O2} : oxygen uptake rate [mmol/L/h]
r_{ATP} : ATP regeneration rate [mmol/L/h]
r_{MeOH} : methanol consumption rate [mmol/L/h]
r_{NADH}^{C} : NADH consumption rate [mmol/L/h], C represents "consumption"
r_{NADH}^{F} : NADH formation rate [mmol/L/h], F represents "formation"

REFERENCES

1. J. L. Cereghino and J. M. Cregg, *FEMS Microbiol. Rev.*, **24**, 45 (2000).
2. S. Macauley-Patrick, M. L. Fazenda, B. McNeil and L. M. Harvey, *Yeast*, **22**, 249 (2005).
3. H. W. Chang, C. R. Jeng, J. J. Liu, T. L. Lin, C. C. Chang, M. Y. Chia, Y. C. Tsai and V. F. Pang, *Vet. Microbiol.*, **108**, 167 (2005).
4. J. Chinsangaram, M. P. Moraes, M. Koster and M. J. Grubman, *J. Virol.*, **77**, 1621 (2003).
5. G. P. Cereghino, J. L. Cereghino, C. Ilgen and J. M. Cregg, *Curr. Opin. Biotechnol.*, **13**, 329 (2002).
6. T. Zhang, F. Gong, Y. Peng and Z. M. Chi, *Process. Biochem.*, **44**, 1335 (2009).
7. N. K. Khatri and F. Hoffmann, *Biotechnol. Bioeng.*, **93**, 871 (2006).
8. A. Nakano, C. Y. Lee, A. Yoshida, T. Matsumoto, N. Shiomi and S. Katoh, *J. Biosci. Bioeng.*, **101**, 227 (2006).
9. H. F. Hang, W. Chen, M. J. Guo, J. Chu, Y. P. Zhuang and S. L. Zhang, *Korean J. Chem. Eng.*, **25**, 1065 (2008).
10. B. E. Mayson, D. G. Kilburn, B. L. Zamost, C. K. Raymond and G. J. Lesnicki, *Biotechnol. Bioeng.*, **81**, 291 (2003).
11. M. Jahic, J. C. Rotticci-Mulder, M. Martinelle, K. Hult and S.-O. Enfors, *Bioprocess Biosyst. Eng.*, **24**, 385 (2002).
12. R. S. Yu, S. J. Dong, Y. M. Zhu, H. Jin, M. J. Gao, Z. Y. Duan, Z. Y. Zheng, Z. P. Shi and Z. Li, *Bioprocess Biosyst. Eng.*, **33**, 473 (2010).
13. Y. Wang, Z. H. Wang, Q. L. Xu, G. C. Du, Z. Z. Hua, L. M. Liu, J. H. Li and J. Chen, *Process. Biochem.*, **44**, 949 (2009).
14. C. Y. Lee, S. J. Lee, K. H. Jung, S. Katoh and E. K. Lee, *Process Biochem.*, **38**, 1147 (2003).
15. C. Jungo, I. Marison and U. von Stockar, *J. Biotechnol.*, **130**, 236 (2007).
16. M. Dragosits, J. Stadlmann, J. Albiol, K. Baumann, M. Maurer, B. Gasser, M. Sauer, F. Altmann, P. Ferrer and D. Mattanovich, *J. Proteome Res.*, **8**, 1380 (2009).
17. H. L. Zhao, C. Xue, Y. Wang, X. Q. Yao and Z. M. Liu, *Appl. Microbiol. Biotechnol.*, **81**, 235 (2008).
18. M. Jahic, F. Wallberg, M. Bollok, P. Garcia and S.-O. Enfors, *Microb. Cell Fact.*, **2**, 6 (2003).
19. J. G. Zhang, X. D. Wang, J. N. Zhang and D. Z. Wei, *J. Biosci. Bioeng.*, **105**, 335 (2008).
20. S. H. Woo, S. H. Park, H. K. Lim and K. H. Jung, *J. Ind. Microbiol. Biotechnol.*, **32**, 474 (2005).
21. P. Li, A. Anumanthan, X. G. Gao, K. Ilangovan, V. V. Suzara, N. Düzgünes and V. Renugopalakrishnan, *Appl. Biochem. Biotechnol.*, **142**, 105 (2007).
22. S. Suye, A. Ogawa, S. Yokoyama and A. Obayashi, *Agric. Biol. Chem.*, **54**, 1297 (1990).
23. S. B. Duan, Z. P. Shi, H. J. Feng, Z. Y. Duan and Z. G. Mao, *Biochem. Eng. J.*, **30**, 88 (2006).
24. H. Jin, Z. Y. Zheng, M. J. Gao, Z. Y. Duan, Z. P. Shi, Z. X. Wang and J. Jin, *Biochem. Eng. J.*, **37**, 26 (2007).
25. T. Charoenrat, M. Ketudat-Cairns, H. Stendahl-Andersen, M. Jahic and S.-O. Enfors, *Bioprocess Biosyst. Eng.*, **27**, 399 (2005).
26. K. Schroer, K. Peter Luef, F. Stefan Hartner, A. Glieder and B. Pscheidt, *Metab. Eng.*, **12**, 8 (2010).
27. I. J. van der Klei, H. Yurimoto, Y. Sakai and M. Veenhuis, *Biochim. Biophys. Acta*, **12**, 1453 (2006).